

Non-LTE Calculation of Sunspot Spectra  
Based on Optically-Thick Semiempirical Modeling

Eugene H. Avrett

Harvard-Smithsonian Center for Astrophysics

Collaborators: H. Tian, E. Landi, W. Curdt, J.-P Wuelser

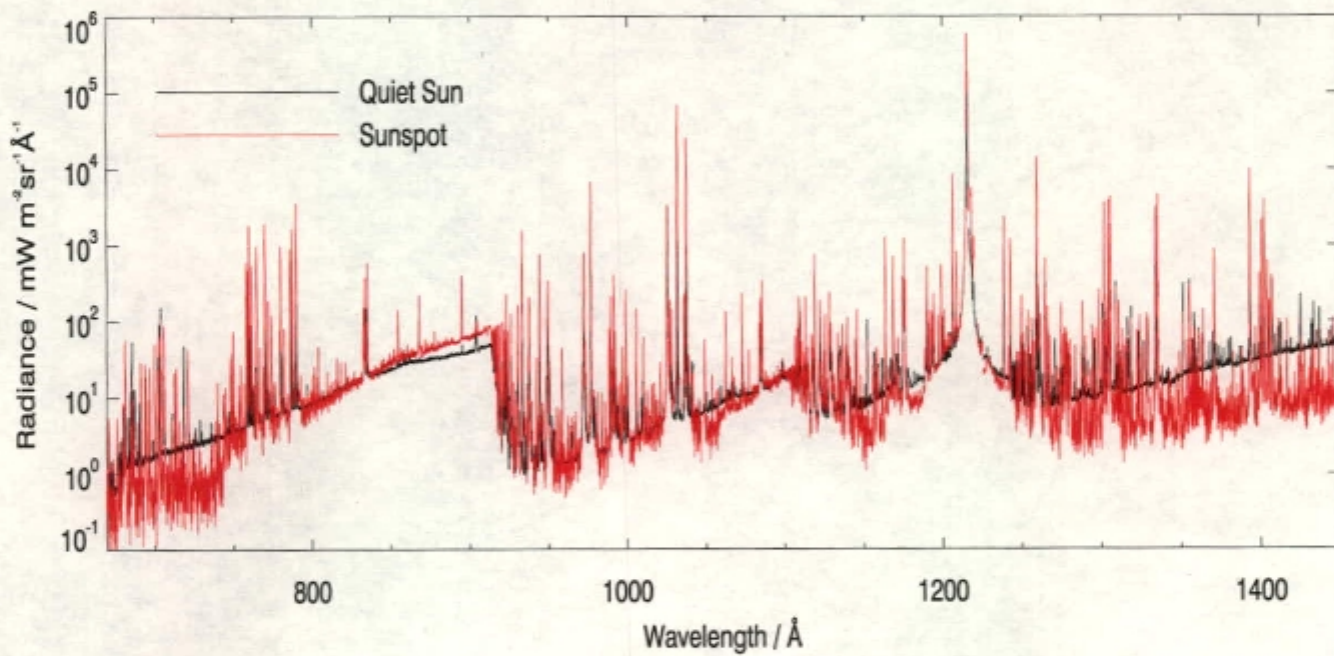


Fig. 1.— caption

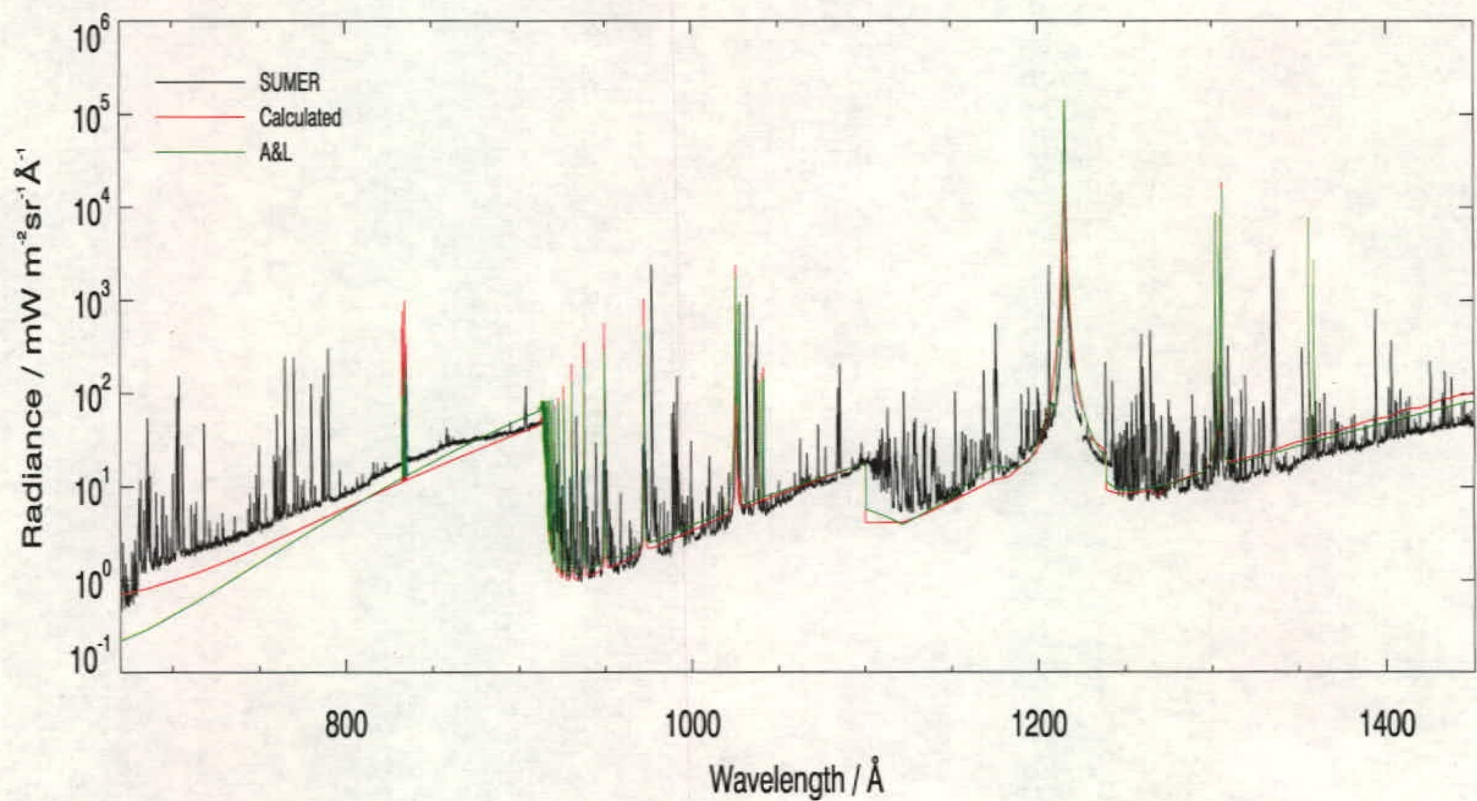


Fig. 2.— caption

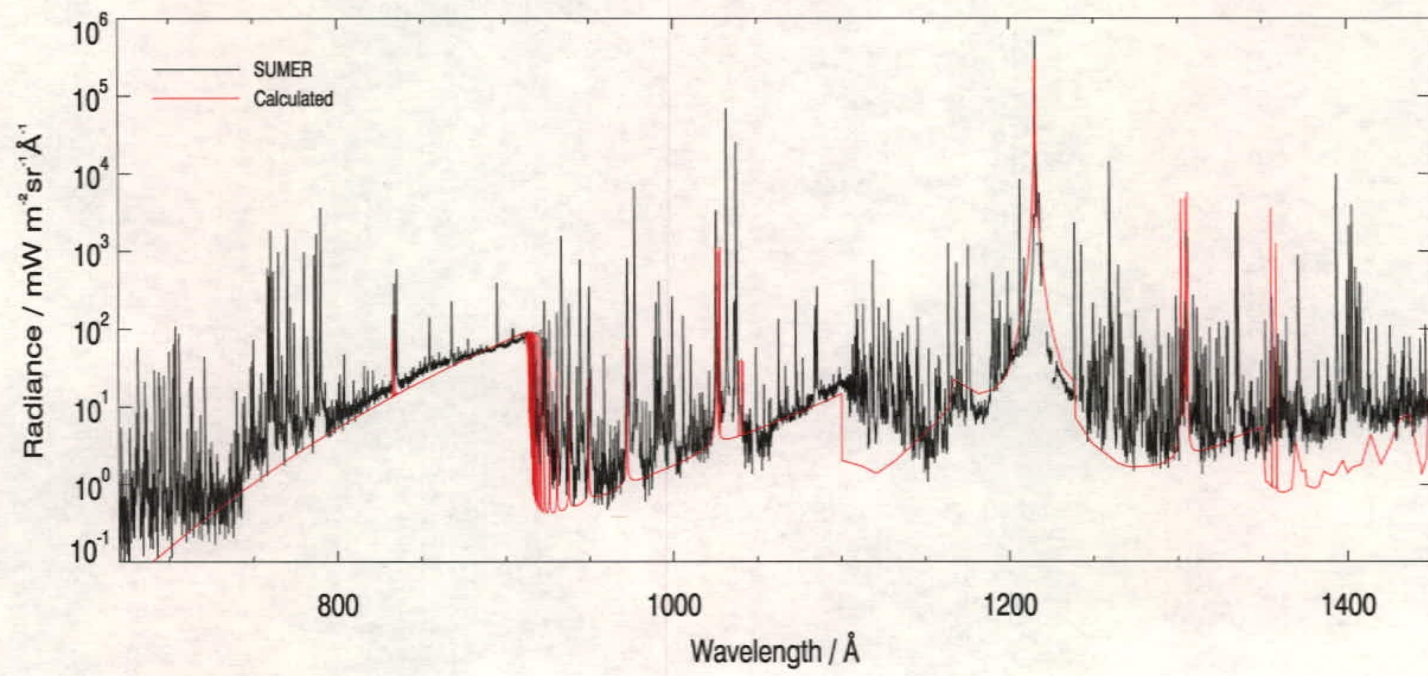
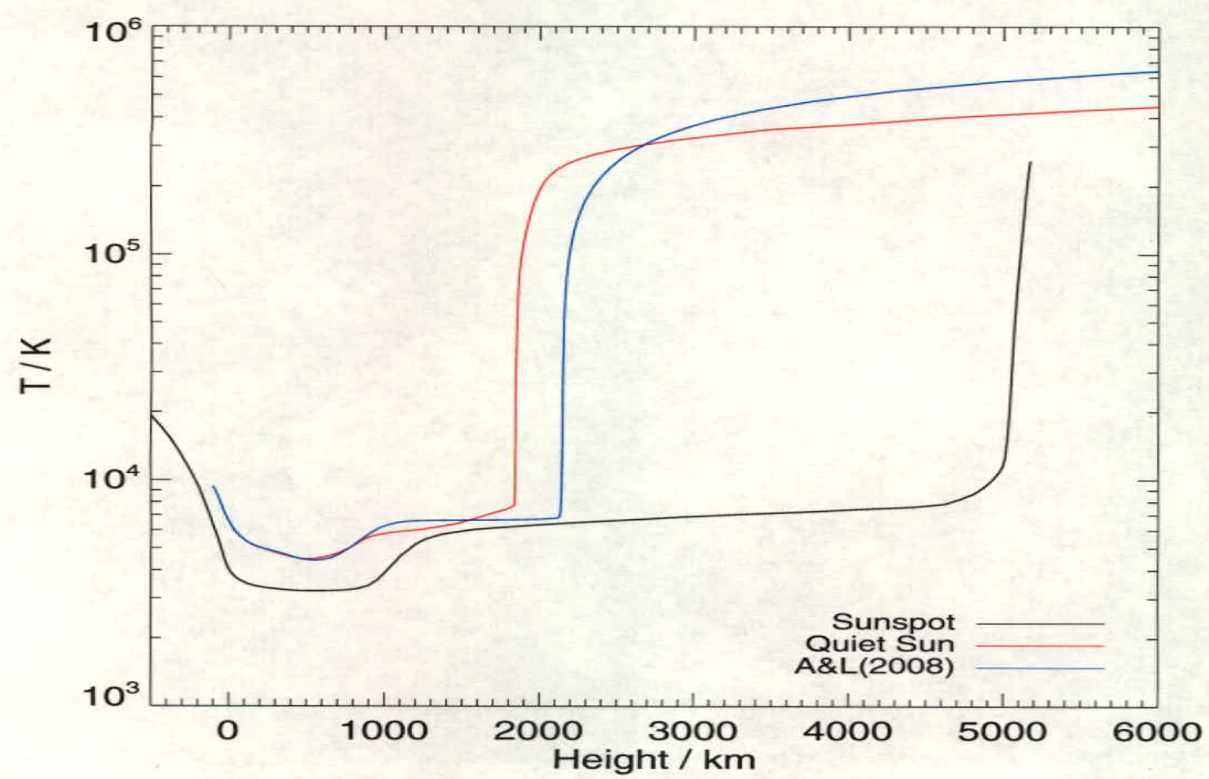


Fig. 3.— caption



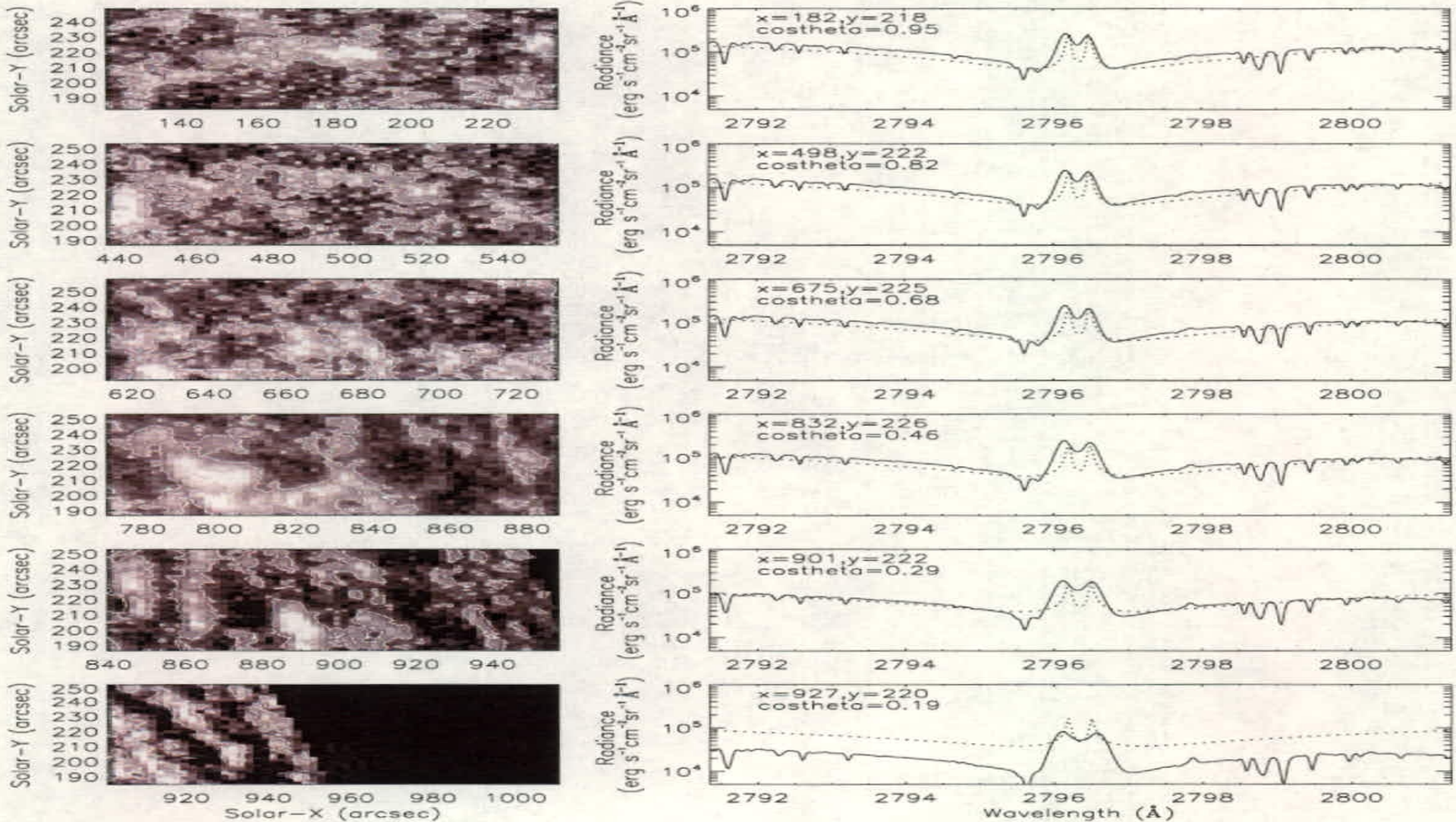


Fig. 4.— **Left::** Mg II wind images integrated over the 2791.35–2792.63 Å wavelength range at different  $\mu$  angles. The contours outline the sunspot umbra. **Right:** IRIS Mg II k line profiles average within the contours (solid lines) are compared with the model output of the quiet Sun (dotted and dashed lines). The coordinates (x,y) and  $\mu$  values ( $\cos\theta$ ) are also marked in the right panels.

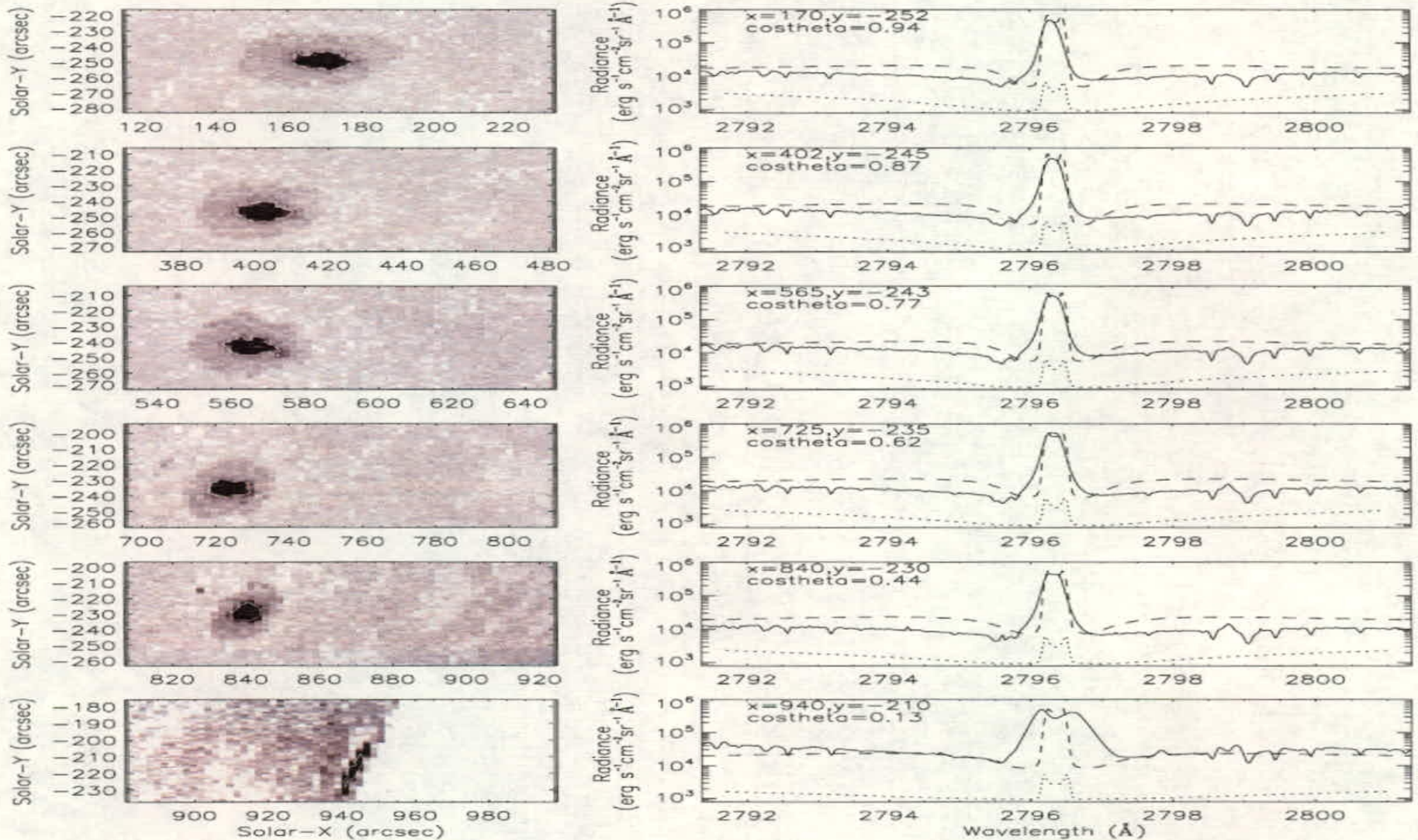


Fig. 5.— Mg II wind images at different  $\mu$  angles. The contours outline the quiet Sun network. **Right:** IRIS Mg II k line profiles averaged within the contours (solid lines) are compared with model output (dotted lines). The coordinates (x,y) and  $\mu$  values ( $\cos \theta$ ) are also marked in the right panels.

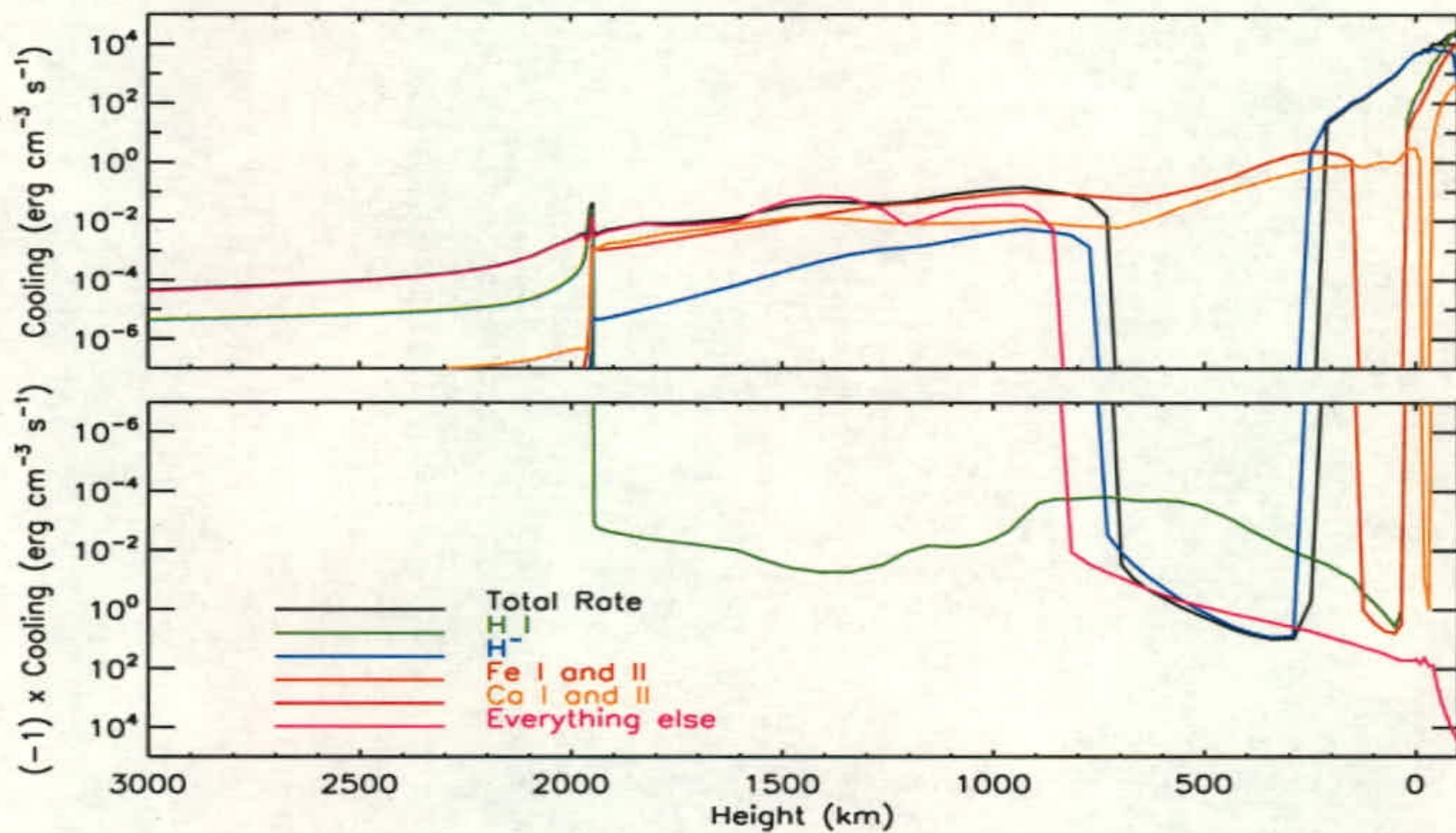


Fig. 6.— Total calculated net radiative cooling rate for the quiet Sun, and the contributions from Hydrogen,  $H^-$ , calcium, iron, and everything else.

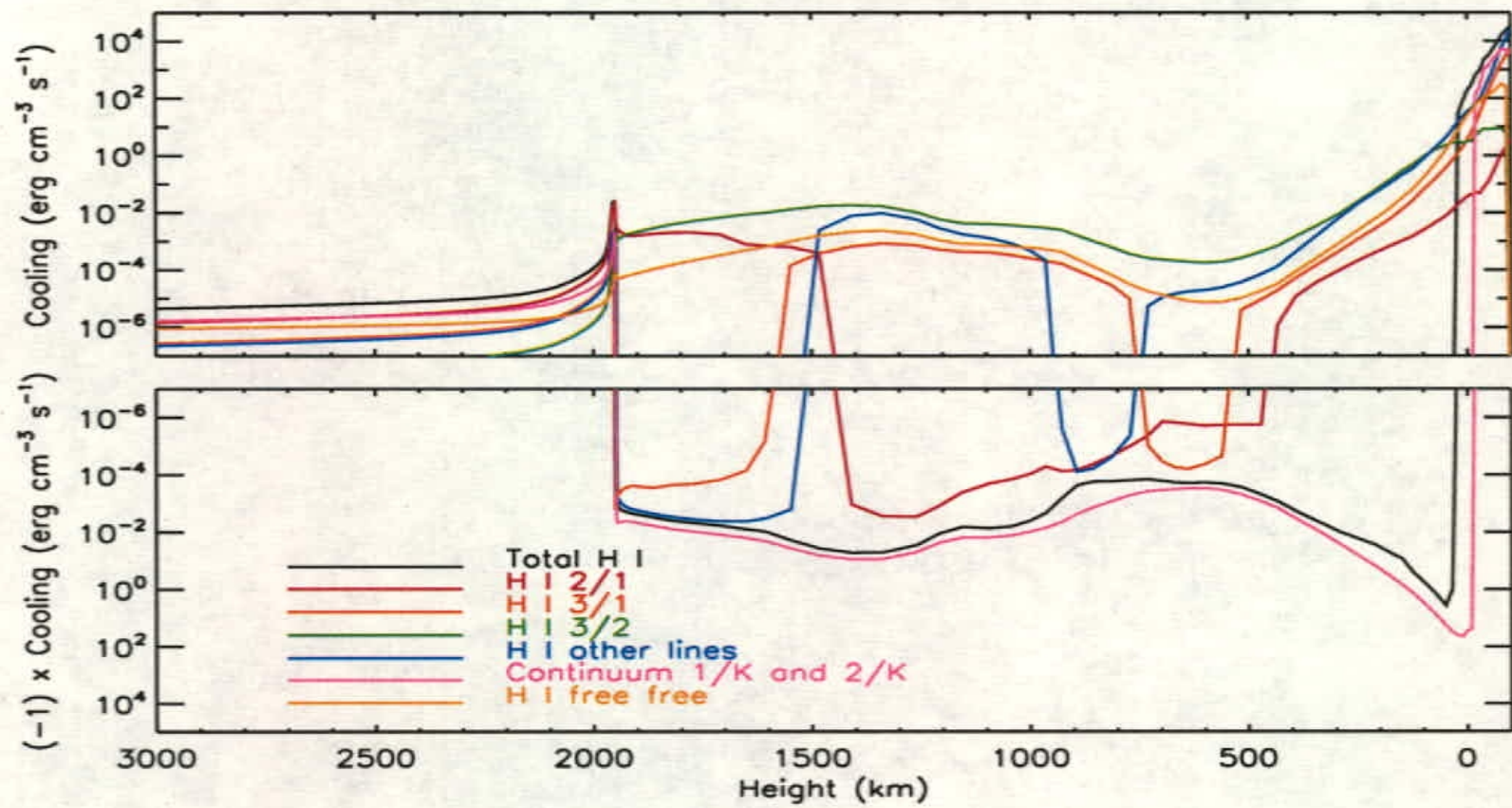


Fig. 7.— The components of the Hydrogen rate for the quiet Sun.

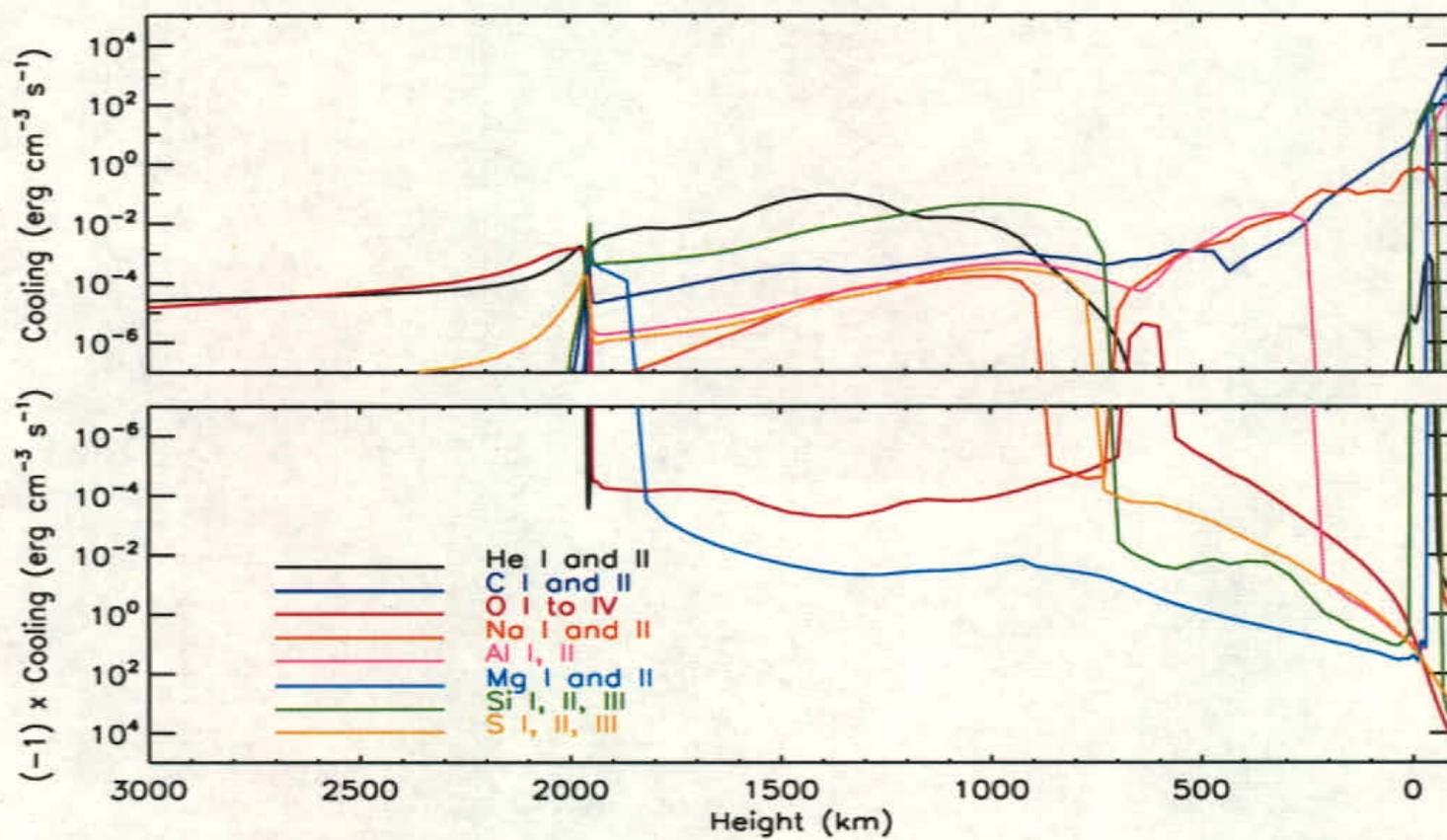


Fig. 8.— The other contributions for the quiet Sun: He<sub>I,II</sub>, C<sub>I,II</sub>, O<sub>I-IV</sub>, Na<sub>I,II</sub>, Mg<sub>I,II</sub>, Al<sub>I,II</sub>, Si<sub>I-III</sub>, and S<sub>I-III</sub>.

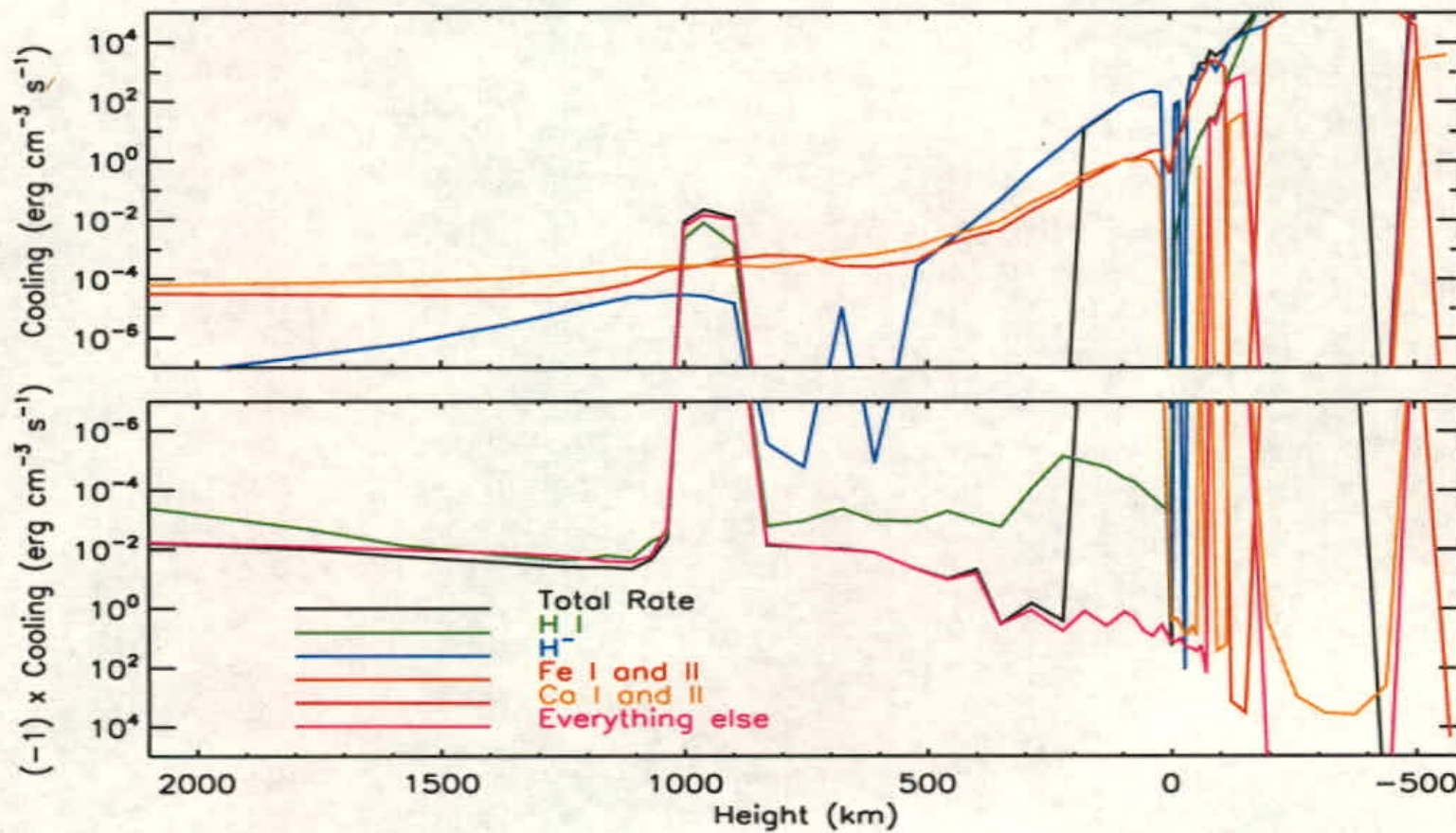


Fig. 9.— Total calculated net radiative cooling rate for the sunspot, and the contributions from Hydrogen,  $\text{H}^-$ , calcium, iron, and everything else.

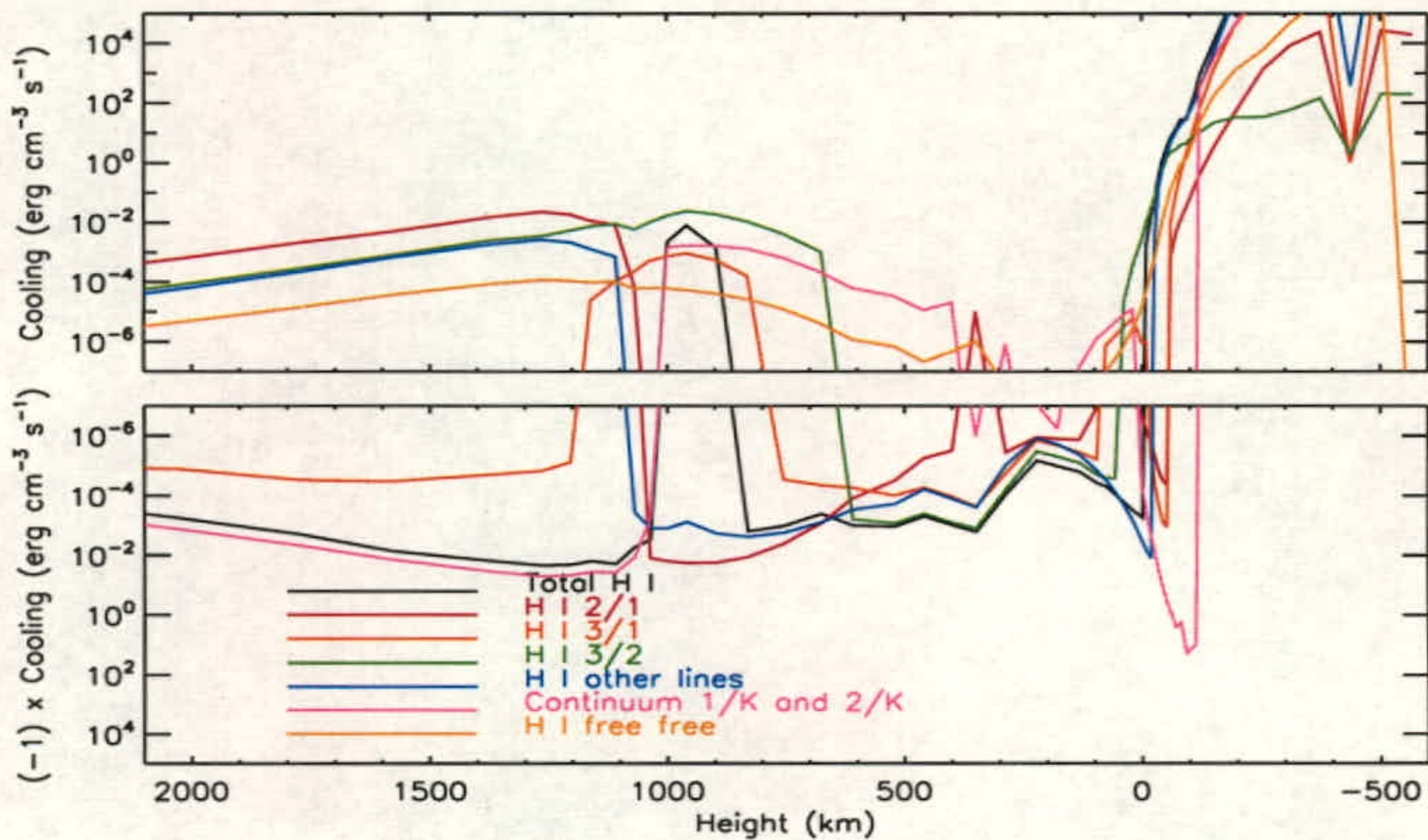


Fig. 10.— The components of the Hydrogen rate for the sunspot.

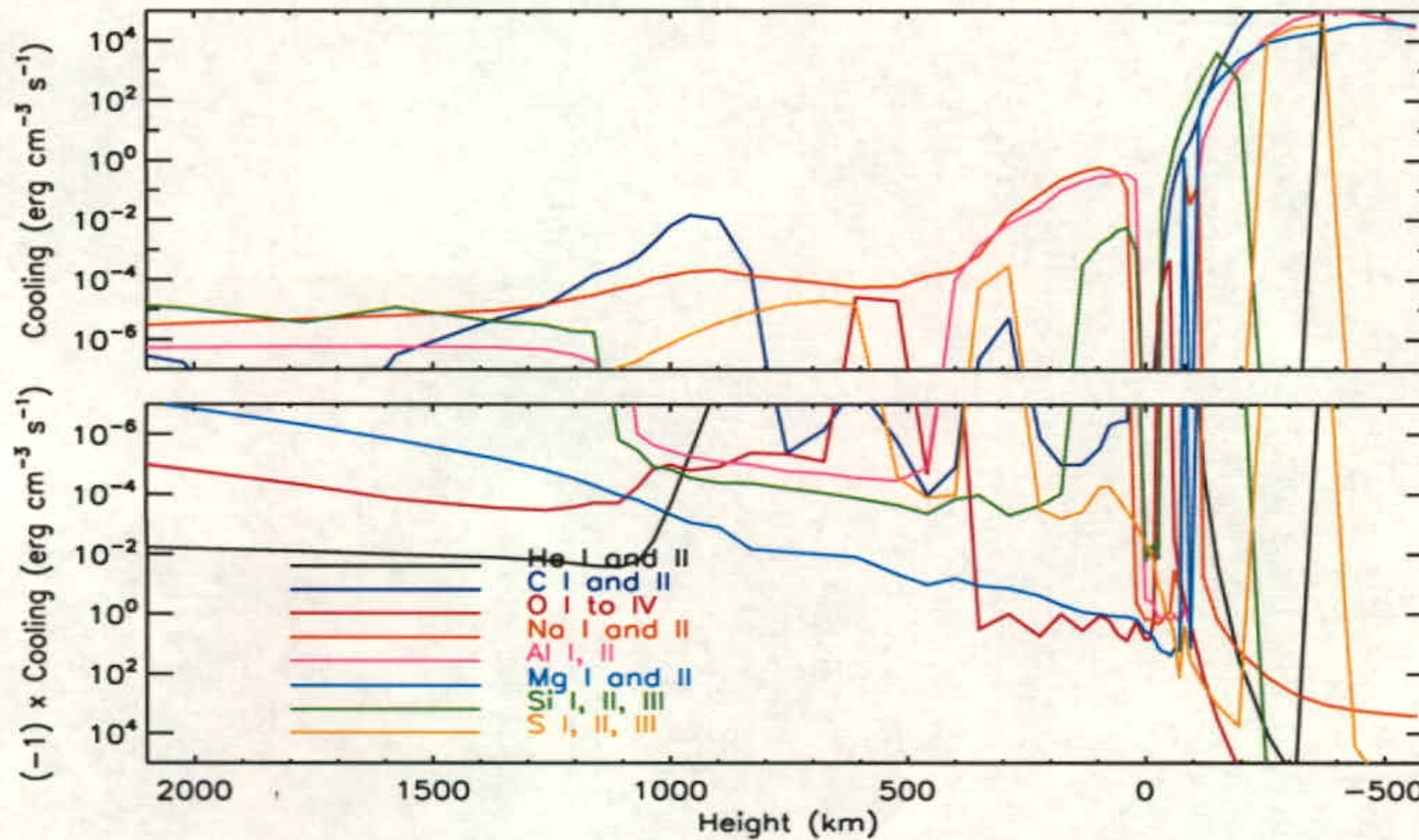


Fig. 11.— The other contributions for the sunspot: He I,II, C I,II, O I-IV, Na I,II, Mg I,II, Al I,II, Si I-III, and Si I-III.